Distinct Orogenic Processes in the South- and North-Central Tien Shan From Receiver Functions

Xuewei Bao[1], Bingfeng Zhang[1] & Yixian Xu[1]
[1]Zhejiang University, School of Earth Sciences, Key Laboratory of Geoscience Big Data and Deep Resource of Zhejiang Province

Introduction

Uplifting mechanisms for **the Tien Shan**, one of the largest and most active intracontinental orogenic belts on Earth, have been under debate for decades, a key issue being **how the convergence has been accommodated at depth**. The underthrusting of the Tarim and Kazakh lithosphere beneath the Tien Shan has been proposed based on several geophysical findings (e.g. Lei, 2011). However, such hypothesis remains controversial, since a deep seismic-reflection profile in the Central Tien Shan (Gao et al., 2013) and a recent receiver function (RF) investigation in the Eastern Tien Shan (Li, Zhang, et al., 2016) show no clear evidence for the northward underthrusting of the Tarim Basin.

In order to deepen our understanding of the orogenic processes in the Tien Shan, **RFs derived from an orogen-perpendicular array of closely spaced seismograph stations are used to image the Moho with unprecedented details**, offering fresh insights into the deformation patterns of compressional intracontinental orogens **(Zhang et al., 2020).**

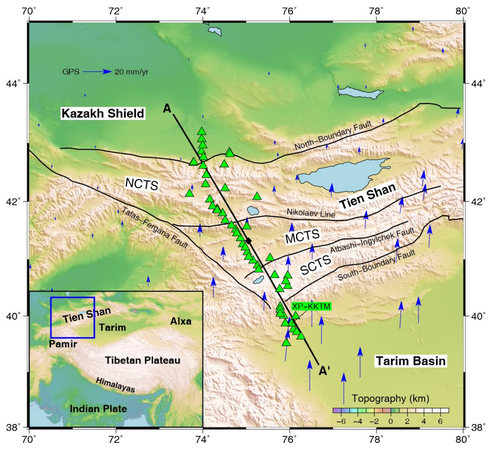

Figure 1. Topography map of the Central Tien Shan. Black thin lines show major fault zones and sutures separating main tectonic segments: the North-Central Tien Shan (NCTS), the Middle-Central Tien Shan (MCTS), and the South-Central Tien Shan (SCTS). Stations are marked as green triangles. Line A-A' shows the projected profile in Figure 2 and Figure 4. the bottom left panel shows the study area in a larger scale. Blue arrows denote GPS velocities relative to Eurasia (Zubovich et al., 2010).

Data and Methods

Receiver function calculation

Data: MANAS, KNET, KRNET, GHENGIS;
Events: 30°<Δ< 95°, M_b>5.5, High SNR;
Quality control: misfit>0.7, visual selection;

A total of 9247 RFs are obtained.

Method 1: CCP stacking

Common-conversion-point (CCP) stacking (Zhu et al., 2006) projects every amplitude on the RFs into the depth domain along the theoretical ray path determined using the background velocity model. The existence and properties of seismic discontinuities are detected based on the conversion amplitudes that depend on the magnitudes and signs of velocity contrasts.

Method 2: H-k-c stacking

H-k-c stacking (Li et al., 2019) resolves and removes the degree-1 and degree-2 back-azimuthal harmonic variations of Moho Ps and two crustal multiples and then performs the traditional H-k scheme on the harmonic-corrected RFs to calculate the optimal solution of crustal thickness (H) and Vp/Vs ratio (k).

phase arrival

$$H = \frac{t_{Ps}}{\sqrt{1/V_s^2 - p^2} - \sqrt{1/V_p^2 - p^2}} = \frac{t_{PpPs}}{\sqrt{1/V_s^2 - p^2} + \sqrt{1/V_p^2 - p^2}} = \frac{t_{PpSs+PsPs}}{2\sqrt{1/V_s^2 - p^2}}$$

Harmonic variations

$$F(\theta) = A_0 + A_1\cos(\theta - \theta_1) - A_2\cos 2(\theta - \theta_2)$$

Morphology of the Moho Discontinuity

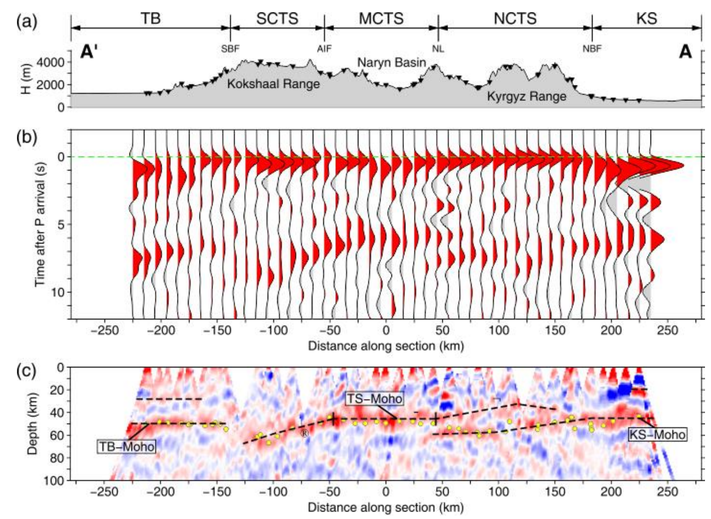

① **KS:** ~45-km Moho
② **NTS:** Moho doublet
③ **MTS:** ~46-km, flat Moho
④ **STS:** diffuse Moho, dip southward to ~65-km depth
⑤ **TB:** ~50-km, flat and sharp Moho & Moho offset beneath SBF

Figure 2. (a) Surface relief along profile A-A'. (TB: the Tarim Basin, SCTS: the South-Central Tien Shan, MCTS: the Middle-Central Tien Shan, NCTS: the North-Central Tien Shan, KS: the Kazakh Shield, SBF: South-Boundary Fault, AIF: Atbashi-Ingylchek Fault, NL: Nikolaev Line, and NBF: North-Boundary Fault). (b) Stacked receiver function image. (c) Image showing the CCP results. Moho depths obtained by H-k-c analysis are marked by yellow circles. Black dashed lines denote the preferred Moho geometry.

Crustal Thickness and Vp/Vs Ratio

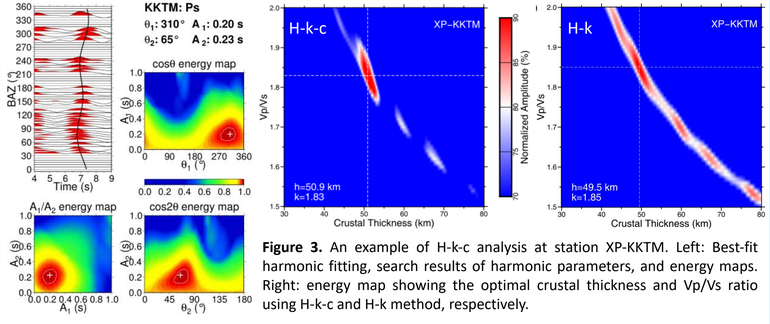

Figure 3. An example of H-k-c analysis at station XP-KKTM. Left: Best-fit harmonic fitting, search results of harmonic parameters, and energy maps. Right: energy map showing the optimal crustal thickness and Vp/Vs ratio using H-k-c and H-k method, respectively.

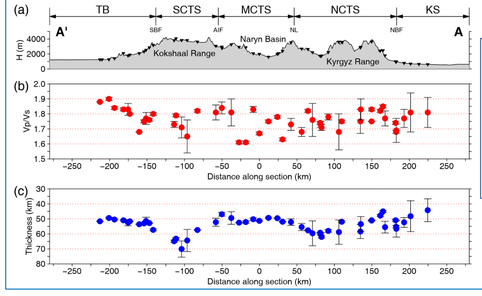

The ambiguity on the energy maps is greatly reduced due to the removal of harmonic effects.

① **Crustal thickness:** 44-70 km
② **Vp/Vs ratio:** 1.61-1.90

Figure 4. crustal thickness and Vp/Vs ratio measurements from H-k-c analysis.

Discussion and Conclusions

- Detailed crustal structure beneath the Central Tien Shan is imaged, suggesting **varying deformation processes perpendicular to its strike**.
- A southward-dipping diffuse Moho is imaged in the **SCTS** in contrast with the relatively flat and sharp Moho beneath the Tarim Basin. This feature along with the large Moho offset beneath the South-Boundary Fault suggests that **the shortening and thickening of the Tien Shan crust rather than the underthrusting of the Tarim Basin** are responsible for the uplift of the SCTS.
- The Moho doublet in the **NCTS** provides direct evidence for **the low-angle southward underthrusting of the Kazakh lower crust** contributing to the uplift there. The lower crustal conversion at 30-40 depth beneath the NCTS marks the upper bound of a high-velocity layer.
- Relatively flat Moho and low surface relief in the **MCTS** suggest that this region **has experienced minor deformation in the Cenozoic**, thus forming the sedimentary basin.
- **A total crustal shortening of ~130 km** is estimated by the imaged Moho morphology. In detail, ~110 km is accommodated by the Moho overlap in the NCTS while ~20 km is absorbed in the SCTS by crustal thickening.

References

1. Gao, R., Hou, H., Cai, X., Knapp, J. H., He, R., Liu, J., et al. (2013). Fine crustal structure beneath the junction of the Southwest Tian Shan and Tarim Basin, NW China. Lithosphere, 5(4), 382–392. https://doi.org/10.1130/l248.1
2. Lei, J. (2011).Seismic tomographic imaging of the crust and upper mantle under the central and western Tien Shan orogenic belt. Journal of Geophysical Research, 116, B09305. https://doi.org/10.1029/2010jb008000
3. Li, J., Song, X., Wang, P., & Zhu, L. (2019). A generalized H-κ method with harmonic corrections on Ps and its crustal multiples in receiver functions. Journal of Geophysical Research: Solid Earth, 124, 3782–3801. https://doi.org/10.1029/2018jb016356
4. Li, J., Zhang, J., Zhao, X., Jiang, M., Li, Y., Zhu, Z., et al. (2016). Mantle subduction and uplift of intracontinental mountains: A case study from the Chinese Tianshan Mountains within Eurasia. Scientific Reports, 6(1), 1–8. https://doi.org/10.1038/srep28831
5. **Zhang, B., Bao, X., & Xu, Y. (2020). Distinct orogenic processes in the south- and north-central tien shan from receiver functions. Geophysical Research Letters, 47, e2019GL086941. https://doi.org/10.1029/2019GL086941**
6. Zhu, L., Mitchell, B. J., Akyol, N., Cemen, I., & Kekovali, K. (2006). Crustal thickness variations in the Aegean region and implications for the extension of continental crust. Journal of Geophysical Research, 111, B01301. https://doi.org/10.1029/2005jb003770
7. Zubovich, A. V., Wang, X., Scherba, Y. G., Schelochkov, G. G., Reilinger, R., Reigber, C., et al. (2010). GPS velocity field for the Tien Shan and surrounding regions. Tectonics, 29, TC6014. https://doi.org/10.1029/2010tc002772

Acknowledgements

We would like to thank Lupei Zhu and Jiangtao Li for sharing their codes and Xiaodong Song for his constructive comments. Waveform data are archived and provided by IRIS Data Management Center (http://ds.iris.edu/ds/nodes/dmc/). This study is supported by the National Natural Science Foundation of China (41774045 and 41830212) and the Fundamental Research Funds for the Central Universities.

Contact Me!

Xuewei Bao - Research Professor
xwbao@zju.edu.cn

Photography encouraged